

Optimal control theory for maximum power of Brownian heat engines

Jin-Fu Chen^{1,*} and H. T. Quan^{1,2,3,†}

¹*School of Physics, Peking University, Beijing, 100871, China*

²*Collaborative Innovation Center of Quantum Matter, Beijing 100871, China*

³*Frontiers Science Center for Nano-optoelectronics, Peking University, Beijing, 100871, China*

(Dated: October 31, 2023)

The pursuit of achieving the maximum power in microscopic thermal engines has gained increasing attention in recent studies of stochastic thermodynamics. We employ the optimal control theory to study the performance of Brownian heat engines and determine the optimal heat-engine cycles in generic damped situation, which were previously known only in the overdamped and the underdamped limits. These optimal cycles include two isothermal processes, two adiabatic processes, and an extra isochoric relaxation process at the upper stiffness constraint. Our results not only interpolate the optimal cycles between the overdamped and the underdamped limits, but also determine the appropriate friction coefficient of the Brownian heat engine to achieve the maximum power. These findings offer valuable insights for the development of high-performance Brownian heat engines in experimental setups.

Introduction. The output power is an important index to characterize the performance of real heat engines. To achieve efficient energy conversion at the nanoscale, Brownian heat engines were invented to extract useful work by harnessing the fluctuation and dissipation of a single Brownian particle [1–6]. The output power of these microscopic heat engines is significantly influenced by the control protocol of heat-engine cycles. The previous optimization was limited to either the overdamped limit [7–13] or the underdamped limit [14, 15]. In the underdamped limit, the efficiency at the maximum power agrees with Curzon-Ahborn’s prediction [16]. The output power diminishes in the both the overdamped and the underdamped limits. Higher output power is expected in the intermediate coupling regime, however, all the previous methods fails in this regime (see Ref. [14]). Ever since the introduction of Brownian heat engines [8], the optimization of heat-engine cycles beyond the two limits has been an outstanding unsolved problem.

Recently, the thermodynamic geometry [17–21] has been applied to optimize control protocols of thermodynamic processes in the slow-driving regime [22–29]. However, these slow-driving protocols are not necessarily optimal to achieve the maximum power since the optimal heat-engine cycles can be beyond the slow-driving regime. A more elaborate optimization method is to employ the optimal control theory [30]. While extensively employed in other subfields of physics, such as, optimal controls of closed and open quantum systems [31–35] and quantum algorithms [36, 37], the optimal control theory has almost never been applied to study thermodynamic optimization (but see [38, 39]).

In this Letter, we employ the optimal control theory to solve the longstanding problem of Brownian heat engines: determining the optimal cycles and finding the maximum

power of Brownian heat engines in generic damped situation. Our method of determining the optimal cycles is valid for arbitrary friction coefficient. Under given control constraints of the stiffness and the bath temperature, we find a family of cycles with conserved pseudo Hamiltonian, which is introduced by the Pontryagin maximum principle [30]. The optimal cycle is the one with the largest pseudo Hamiltonian promising the maximum power. Our results not only interpolate the known results of the optimal cycles in the overdamped limit [7, 8] and the underdamped limit [14, 15], but also determine the appropriate friction coefficient of the Brownian heat engine to achieve the maximum power. This indicates that the most powerful thermal engines operate at the intermediate coupling regime, neither too weak (underdamped limit) nor too strong (overdamped limit). Our results provide direct guidance for designing and optimizing Brownian heat engines in experimental setups.

Setup and optimal isothermal processes. We consider a microscopic heat engine with a single Brownian particle as the working substance [1, 3, 8, 15]. The Hamiltonian of the system is

$$H = \frac{p^2}{2} + \frac{1}{2}\lambda x^2, \quad (1)$$

where the mass of the particle is set as unity, and the work parameter λ is the stiffness of the harmonic potential. The system is coupled to a heat bath at temperature T_b . The stiffness λ and the bath temperature T_b can be varied by an external agent to construct heat-engine cycles. The evolution of the distribution $\rho(x, p, t)$ of position and momentum is described by the Fokker-Planck equation [40]

$$\frac{\partial \rho}{\partial t} = -\frac{\partial}{\partial x}(p\rho) + \frac{\partial}{\partial p}(\lambda x\rho + \kappa p\rho + \kappa T_b \frac{\partial \rho}{\partial p}), \quad (2)$$

with the friction coefficient κ . The distribution remains Gaussian during the evolution when the system initiates

* chenjinfu@pku.edu.cn

† htquan@pku.edu.cn

from an initial Gaussian state. We characterize the state of the system with the covariances of position and momentum $\Gamma_{xx} = \langle x^2 \rangle$, $\Gamma_{xp} = \langle xp \rangle$, and $\Gamma_{pp} = \langle p^2 \rangle$, which satisfy the following evolution equations [41, 42]

$$\dot{\Gamma}_{xx} = 2\Gamma_{xp}, \quad (3)$$

$$\dot{\Gamma}_{xp} = -\lambda\Gamma_{xx} - \kappa\Gamma_{xp} + \Gamma_{pp}, \quad (4)$$

$$\dot{\Gamma}_{pp} = -2\lambda\Gamma_{xp} - 2\kappa\Gamma_{pp} + 2\kappa T_b. \quad (5)$$

The work performed on the system is $\dot{W} = \dot{\lambda}\Gamma_{xx}/2$. By substituting $\Gamma_{xp} = \dot{\Gamma}_{xx}/2$ and $\Gamma_{pp} = (\kappa\dot{\Gamma}_{xx} + 2\lambda\Gamma_{xx} + \ddot{\Gamma}_{xx})/2$ into Eq. (5), we obtain a high-order differential equation of Γ_{xx} as

$$\ddot{\Gamma}_{xx} + 3\kappa\dot{\Gamma}_{xx} + (2\kappa^2 + 4\lambda)\dot{\Gamma}_{xx} = 4\kappa T_b - (2\dot{\lambda} + 4\kappa\lambda)\Gamma_{xx}. \quad (6)$$

We notice that the system is not fully controllable [30], since there are three state variables Γ_{xx} , Γ_{xp} and Γ_{pp} but only two parameters λ and T_b can be varied. To simplify the optimal control problem, we consider approximate dynamics by neglecting the higher-order derivatives $\ddot{\Gamma}_{xx}$ and $\dot{\Gamma}_{xx}$ in Eq. (6) and obtain

$$\dot{\Gamma}_{xx} = -\frac{2\kappa\lambda}{\kappa^2 + 2\lambda}\left(\Gamma_{xx} - \frac{T_b}{\lambda}\right) - \frac{\dot{\lambda}}{\kappa^2 + 2\lambda}\Gamma_{xx}, \quad (7)$$

which is rewritten in the form of the potential energy $V \equiv \lambda\Gamma_{xx}/2$ as

$$\dot{V} = \frac{(\kappa^2 + \lambda)\dot{\lambda}}{(\kappa^2 + 2\lambda)\lambda}V - \frac{\kappa\lambda(2V - T_b)}{(\kappa^2 + 2\lambda)}. \quad (8)$$

Such approximation renders the system controllable [30]. We will see the approximation works quantitatively well in both the overdamped and the underdamped limits and qualitatively well in the intermediate coupling regime.

We hope to optimize the output power of the cycle. To employ the optimal control theory, we regard the potential energy V and the stiffness λ as state variables. The control parameters are the rate of stiffness change $\alpha = \dot{\lambda}/\lambda$ and the bath temperature T_b constrained by $\lambda_L \leq \lambda \leq \lambda_H$ and $T_L \leq T_b \leq T_H$. The output work of the cycle is $W_{\text{out}} = -\int_0^\tau \alpha V dt$. The pseudo Hamiltonian of the optimal control theory for this system is constructed as [43]

$$\mathcal{H} = -\alpha V + \psi_V \frac{(\kappa^2 + \lambda)\alpha V - \kappa\lambda(2V - T_b)}{\kappa^2 + 2\lambda} + \psi_\lambda \alpha \lambda, \quad (9)$$

where ψ_V and ψ_λ are costate variables. The pseudo Hamiltonian \mathcal{H} is a quantity introduced to derive the optimal control protocol, and should be distinguished from the Hamiltonian H of the system. The evolution of the state variables is generated by $\dot{V} = \partial\mathcal{H}/\partial\psi_V$ (Eq. (8))

and $\dot{\lambda} = \partial\mathcal{H}/\partial\psi_\lambda = \alpha\lambda$. The evolution of the costate variables is generated by

$$\dot{\psi}_V = -\frac{\partial\mathcal{H}}{\partial V} = \alpha - \psi_V \frac{\alpha(\kappa^2 + \lambda) - 2\kappa\lambda}{\kappa^2 + 2\lambda}, \quad (10)$$

$$\dot{\psi}_\lambda = -\frac{\partial\mathcal{H}}{\partial\lambda} = \psi_V \frac{\kappa^2(V(\alpha + 2\kappa) - \kappa T_b)}{(\kappa^2 + 2\lambda)^2} - \alpha\psi_\lambda. \quad (11)$$

The control parameters α and T_b are varied to maximize \mathcal{H} under the control constraints. The control protocol of the bath temperature T_b is determined from

$$\frac{\partial\mathcal{H}}{\partial T_b} = \frac{\kappa\lambda\psi_V}{\kappa^2 + 2\lambda}, \quad (12)$$

which corresponds to a bang-bang control $T_b = T_H$ for $\psi_V > 0$ and $T_b = T_L$ for $\psi_V < 0$. The control protocol of the stiffness change rate α is determined by

$$\frac{\partial\mathcal{H}}{\partial\alpha} = \lambda\psi_\lambda + \frac{V(\kappa^2 + \lambda)\psi_V}{\kappa^2 + 2\lambda} - V. \quad (13)$$

Due to the fact that the right hand side of Eq. (13) does not depend on α , we first consider the singular control with $\partial\mathcal{H}/\partial\alpha = 0$ [30]. The costate variables and the rate of stiffness change are solved as

$$\psi_V = \frac{(\kappa^2 + 2\lambda)(T_b - 2V)}{\lambda T_b + 2\kappa^2 V}, \quad (14)$$

$$\psi_\lambda = \frac{V[2V(2\kappa^2 + \lambda) - \kappa^2 T_b]}{\lambda(\lambda T_b + 2\kappa^2 V)}, \quad (15)$$

$$\alpha = \frac{\kappa\lambda(2V - T_b)[2\kappa^2 V + (\kappa^2 + 2\lambda)T_b]}{V[4\kappa^4 V + 6\kappa^2 \lambda V + (\kappa^2 + 2\lambda)\lambda T_b]}, \quad (16)$$

where Eq. (16) gives the control protocol of isothermal processes.

We eliminate the costate variables with Eqs. (14) and (15), and obtain the pseudo Hamiltonian

$$\mathcal{H} = \frac{\kappa\lambda(T_b - 2V)^2}{\lambda T_b + 2\kappa^2 V}, \quad (17)$$

which reflects the velocity of the control. In quasistatic isothermal processes, the system is in equilibrium with the heat bath, i.e., $V = T_b/2$, and thus $\mathcal{H} = 0$. In non-quasistatic isothermal processes, we can solve V of the optimal control from the conservation of \mathcal{H} as

$$V = \frac{T_b}{2} + \frac{\kappa\mathcal{H}}{4\lambda} \left[1 - \epsilon \sqrt{1 + \frac{4\lambda T_b}{\kappa\mathcal{H}} \left(1 + \frac{\lambda}{\kappa^2} \right)} \right], \quad (18)$$

where $\epsilon = +1$ for expansion process and -1 for compression process.

The control protocol can be significantly simplified in the two limits. In the overdamped limit, the pseudo

Hamiltonian becomes $\mathcal{H} = \lambda(T_b - 2V)^2/(2\kappa V)$, and the control protocol of stiffness and the evolution of potential energy are

$$\lambda(t) = \frac{\lambda_0[1 - \mathcal{H}t/(2V_0)]}{\left(1 + \epsilon\sqrt{\lambda_0\mathcal{H}/(2\kappa V_0)t}\right)^2}, \quad (19)$$

$$V(t) = V_0 - \mathcal{H}t/2. \quad (20)$$

The above protocol agrees with the one obtained in Ref. [7]. In the underdamped limit, the pseudo Hamiltonian becomes $\mathcal{H} = \kappa(T_b - 2V)^2/T_b$. The potential energy V of the optimal control thus remains constant in nonquasistatic isothermal processes

$$V(t) = \frac{T_b}{2} - \frac{\epsilon}{2}\sqrt{\frac{\mathcal{H}T_b}{\kappa}}, \quad (21)$$

and the control protocol is the exponential protocol

$$\frac{\dot{\lambda}}{\lambda} = \frac{2\kappa}{1 - \epsilon\sqrt{\kappa T_b/\mathcal{H}}} = \text{const}, \quad (22)$$

which agrees with the protocol obtained in Refs. [44, 45].

After solving the protocols from Eqs. (8) and (16), we can utilize these protocols to propagate the exact evolution of nonquasistatic isothermal processes by Eqs. (3)-(5). The results are compared and visualized in Fig. 1. We set the bath temperature $T_b = 1$, the friction coefficient $\kappa = 1$, and the initial and final values of stiffness $\lambda(0) = 0.01$ and $\lambda(\tau) = 2000$, and choose four initial values of the potential energy $V(0) = 0.55, 0.75, 0.95$, and 1.15 . With larger $V(0)$, the isothermal compression is completed more rapidly. Figure 1(a) shows the control protocols of the stiffness $\lambda(t)$ (dashed curves). The black dotted curves represent the optimal protocols in the overdamped limit [7, 8] and the underdamped limit [14, 15], matching our protocols at the initial and final stages, respectively. Figure 1(b) shows the evolution of potential energy during isothermal compression processes. The dashed curves are the estimations based on the approximate dynamics, while the solid curves show the exact evolution by Eqs. (3)-(5) with the protocols in Fig. 1(a). The agreement of the solid curves and the dashed curves validates the approximation used in Eq. (7).

Construction of the optimal cycles. We continue to construct heat-engine cycles under the control constraints $\lambda_L \leq \lambda \leq \lambda_H$ and $T_L \leq T_b \leq T_H$. During the whole cycle, the pseudo Hamiltonian is conserved and we thus require two isothermal processes with identical \mathcal{H} . For given \mathcal{H} , we find two switchings associated with the lower and the upper stiffness constraints λ_L and λ_H by simultaneously changing T_b and λ [43]. Thus, \mathcal{H} together with the control constraints determines the control protocol of the cycle.

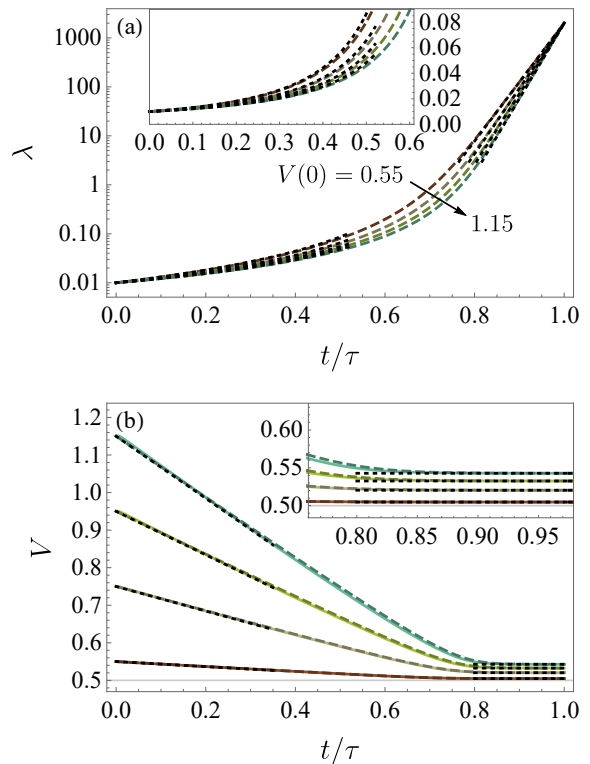


Figure 1. The optimal control of isothermal processes in generic damped situation. (a) The optimal protocols with different control speeds characterized by $V(0) = 0.55, 0.75, 0.95$, and 1.15 . We plot all the protocols (dashed curves) with a rescaled time t/τ with $\lambda(0) = 0.01$ and $\lambda(\tau) = 2000$. (b) The evolution of the potential energy V during the isothermal processes. The solid curves show the results of exact evolution by Eqs. (3)-(5). In both subfigures, the dotted lines show the results in the overdamped and the underdamped limits, and the dashed curves are the results of the approximate dynamics obtained from Eqs. (8) and (16).

The switchings simultaneously change λ and T_b instantaneously, i.e., $\alpha \gg \kappa$, and the evolution equations (8) and (10) are reduced to

$$\dot{V} = \frac{\kappa^2 + \lambda}{\kappa^2 + 2\lambda} \alpha V, \quad (23)$$

$$\dot{\psi}_V = \alpha \left[1 - \frac{(\kappa^2 + \lambda)}{\kappa^2 + 2\lambda} \psi_V \right]. \quad (24)$$

The initial and the final points of the switchings satisfy

$$\frac{V_f \sqrt{\kappa^2 + 2\lambda_f}}{\lambda_i} = \frac{V_i \sqrt{2\lambda_i + \kappa^2}}{\lambda_i}, \quad (25)$$

$$\frac{\lambda_f (\psi_{V_f} - 2) - \kappa^2}{\sqrt{\kappa^2 + 2\lambda_f}} = \frac{\lambda_i (\psi_{V_i} - 2) - \kappa^2}{\sqrt{\kappa^2 + 2\lambda_i}}. \quad (26)$$

The two switchings in a cycle are given by $\lambda_2 \rightarrow \lambda_H, V_2 \rightarrow V_3, \psi_{V_2} \rightarrow \psi_{V_3}$ and $\lambda_5 \rightarrow \lambda_L, V_5 \rightarrow V_6, \psi_{V_5} \rightarrow \psi_{V_6}$, as shown in Fig. 2(a). The six boundary points are

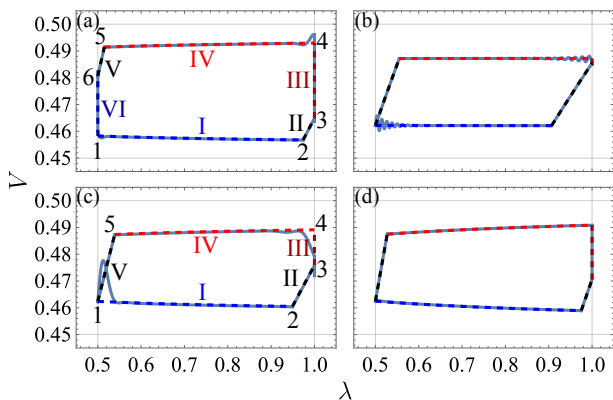


Figure 2. Diagrams of heat-engine cycles. (a) $\kappa = 1$ and $\mathcal{H} = 10^{-4}$ (non-maximum \mathcal{H}), (b) $\kappa = 0.1$ (underdamped), (c) $\kappa = 0.830$ (optimal), and (d) $\kappa = 10$ (overdamped). The control constraints $T_L = 0.9$, $T_H = 1$, $\lambda_L = 0.5$ and $\lambda_H = 1$ are depicted by the horizontal and vertical gray lines. The solid and the dashed curves represent limit cycles of the exact dynamics and the approximate dynamics, respectively.

$l = 1, 2, \dots, 6$, and the six processes I, II, ..., VI. The two switchings are solved from the conservation of \mathcal{H} [43]. With \mathcal{H} large enough, the lower switching connects the two isothermal processes directly without reaching the lower stiffness constraint λ_L . By increasing \mathcal{H} , point 6 will approach point 1 on the cold isothermal curve. Since larger \mathcal{H} leads to higher output power, we consider the maximum \mathcal{H} such that the cycle still reaches λ_L . The output power P of the maximum- \mathcal{H} cycle is evaluated as

$$P = -\frac{W_I + W_{II} + W_{IV} + W_V}{\tau_I + \tau_{II} + \tau_{IV}}. \quad (27)$$

The expressions of the work and the operation time of each process are given in [43].

With the above protocol of a whole cycle, we can propagate Eqs. (3)-(5) and obtain the exact output power of the limit cycle. In accordance with Eq. (27), we choose the connecting processes to be thermodynamic adiabatic (unitary) processes that satisfy $\Gamma_{pp}^f \Gamma_{xx}^f = \Gamma_{pp}^i \Gamma_{xx}^i$. In principle, such unitary evolution can be completed in arbitrary short time by choosing a large Hamiltonian [46, 47]. The corresponding protocol to vary the Hamiltonian can be realized by the shortcut to adiabaticity [48, 49]. After solving Γ_{xx} , Γ_{xp} , and Γ_{pp} for the whole cycle, we also use Eq. (27) to evaluate the exact output power, where the work in each process is evaluated from the exact evolution.

We show diagrams of heat-engine cycles in Fig. 2 for a non-maximum- \mathcal{H} cycle with (a) $\kappa = 1$ and $\mathcal{H} = 10^{-4}$, and three maximum- \mathcal{H} cycles with (b) $\kappa = 0.1$ (underdamped), (c) $\kappa = 0.830$ (optimal), and (d) $\kappa = 10$ (overdamped). Although the exact evolution (solid curves) deviates from the evolution based on the approximate dynamics (dashed curves), our protocols still lead to high output power in the intermediate coupling regime. In the

underdamped limit (Fig. 2(b)), the microscopic heat engine fulfills all the preconditions of the Curzon-Ahlborn engine [15, 16], where the effective temperature of the Brownian particle remains constant ($V = \text{const}$) during isothermal processes [15, 16].

Maximum power of Brownian heat engines. For a given friction coefficient κ , we evaluate the output power P of maximum- \mathcal{H} cycles. Furthermore, the friction coefficient κ can be adjusted to achieve the maximum power. In generic damped situation, we solve the maximum- \mathcal{H} cycle numerically. Analytical results are obtained in the overdamped limit and the underdamped limit.

In the overdamped limit $\kappa^2 \gg \lambda_H$, the cooling rate according to Eq. (8) is equal to $2\lambda/\kappa$. Thus, the output power is inversely proportional to the friction coefficient $P_{\text{over}} \propto 1/\kappa$ [43]. We can choose λ_L as large as possible so that the maximum power P_{over}^* can be achieved by the sliced cycles [43]

$$P_{\text{over}}^* = \frac{\lambda_H T_H}{\kappa} \phi\left(\frac{T_L}{T_H}\right), \quad (28)$$

where $\phi(\theta)$ is the positive root of the polynomial

$$\phi^3 + (11 - 3\theta)\phi^2 + (3\theta^2 + 14\theta - 1)\phi - (\theta - 1)^2\theta = 0, \quad (29)$$

with $\theta = T_L/T_H$. A detailed discussion of these sliced cycles is left in [43].

In the underdamped limit $\kappa^2 \ll \lambda_L$, the maximum power is [14, 15]

$$P_{\text{under}}^* = \frac{\kappa T_H}{4} \left(1 - \sqrt{\frac{T_L}{T_H}}\right)^2, \quad (30)$$

which is proportional to the square of the Curzon-Ahlborn efficiency $\eta_{\text{CA}} = 1 - \sqrt{T_L/T_H}$ [16]. We left the derivations of Eqs. (28) and (30) in [43].

Figure 3 presents the output power P of maximum- \mathcal{H} cycles as a function of the friction coefficient κ . We set the control constraints $T_H = 1$, $T_L = 0.9$, and $\lambda_H = 1$, and choose the lower stiffness constraint $\lambda_L = 1/8$ (blue), $1/4$ (red), $1/2$ (green). The output power of the exact dynamics (dots) agrees well with that of the approximate dynamics (solid curves), and is bounded by the maximum power of sliced cycles (dotted curve) [43]. The maximum power of sliced cycles agrees with Eqs. (28) and (30) in the overdamped and the underdamped limits. The gray horizontal line shows the bound of the output power P_{bound} with the appropriate friction coefficient which leads to the maximum power [43].

Conclusion. The maximum power of Brownian heat engines in the overdamped and the underdamped limits has been obtained previously [7, 8, 14, 15], but how to reach the maximum power in the intermediate coupling regime (generic damped situation) has been a long-standing problem. Previous methods fail in this regime due to the lack of timescale separation.

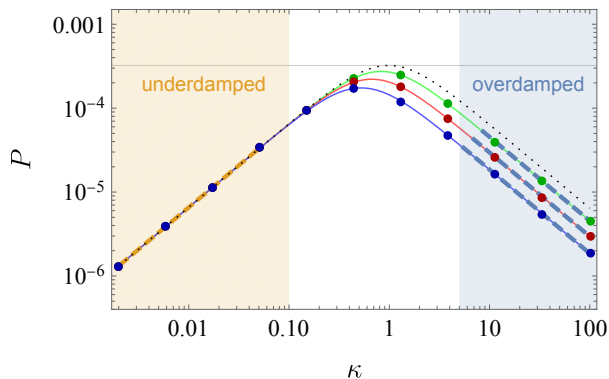


Figure 3. Output power of the optimal cycles with different friction coefficients. We fix the parameters $T_L = 0.9$, $T_H = 1$, $\lambda_H = 1$, and choose different lower stiffness constraints $\lambda_L = 1/8$ (blue), $1/4$ (red), $1/2$ (green). The dots and the solid curves show the results of the exact dynamics [Eqs. (3)-(5)] and the approximate dynamics [Eq. (8)], respectively. The maximum power in the overdamped and the underdamped limits is shown with the right and left dashed lines. The dotted curve shows the maximum power of sliced cycles, and the gray horizontal line shows the bound of the output power P_{bound} with the appropriate friction coefficient.

In our current investigation, we have employed the op-

timal control theory to study the performance of Brownian heat engines to achieve the maximum power. We construct the optimal cycles in generic damped situation. These optimal cycles include two isothermal processes, two adiabatic processes, and an extra isochoric relaxation process at the upper stiffness constraint. We also determine appropriate friction coefficient to achieve the maximum power. This indicates that powerful thermal engines operate at the intermediate coupling regime, neither the weak coupling regime (underdamped limit) nor the strong coupling regime (overdamped limit). This argument should also be valid for quantum heat engines [50–52].

Our findings show the effectiveness of the optimal control theory in thermodynamic optimization, and provide practical guidance for the experimental design and optimization of Brownian heat engines. It is interesting to explore the trade-off relation between the efficiency and output power of Brownian heat engines in generic damped situation and also the optimal protocol of cycles to achieve the maximum power at a given efficiency [25, 53–57], and we leave this for future investigation.

Acknowledgment. This work is supported by the National Natural Science Foundation of China (NSFC) under Grants No. 12147157, No. 11775001 and No. 11825501, No. 12375028.

-
- [1] V. Blickle and C. Bechinger, Realization of a micrometre-sized stochastic heat engine, *Nat. Phys.* **8**, 143 (2012).
 - [2] P. A. Quinto-Su, A microscopic steam engine implemented in an optical tweezer, *Nat. Commun.* **5**, 5889 (2014).
 - [3] I. A. Martínez, É. Roldán, L. Dinis, D. Petrov, J. M. R. Parrondo, and R. A. Rica, Brownian Carnot engine, *Nat. Phys.* **12**, 67 (2016).
 - [4] S. Krishnamurthy, S. Ghosh, D. Chatterji, R. Ganapathy, and A. K. Sood, A micrometre-sized heat engine operating between bacterial reservoirs, *Nat. Phys.* **12**, 1134 (2016).
 - [5] I. A. Martínez, É. Roldán, L. Dinis, and R. A. Rica, Colloidal heat engines: a review, *Soft Matter* **13**, 22 (2017).
 - [6] V. Holubec and A. Ryabov, Fluctuations in heat engines, *J. Phys. A: Math. Theor.* **55**, 013001 (2021).
 - [7] T. Schmiedl and U. Seifert, Optimal finite-time processes in stochastic thermodynamics, *Phys. Rev. Lett.* **98**, 108301 (2007).
 - [8] T. Schmiedl and U. Seifert, Efficiency at maximum power: An analytically solvable model for stochastic heat engines, *Europhys. Lett.* **81**, 20003 (2007).
 - [9] P. R. Zulkowski and M. R. DeWeese, Optimal control of overdamped systems, *Phys. Rev. E* **92**, 032117 (2015).
 - [10] C. A. Plata, D. Guéry-Odelin, E. Trizac, and A. Prados, Optimal work in a harmonic trap with bounded stiffness, *Phys. Rev. E* **99**, 012140 (2019).
 - [11] K. Proesmans, J. Ehrich, and J. Bechhoefer, Finite-Time Landauer Principle, *Phys. Rev. Lett.* **125**, 100602 (2020).
 - [12] Z. Ye, F. Cerisola, P. Abiuso, J. Anders, M. Perarnau-Llobet, and V. Holubec, Optimal finite-time heat engines under constrained control, *Phys. Rev. Research* **4**, 043130 (2022).
 - [13] G.-H. Xu, C. Jiang, Y. Minami, and G. Watanabe, Relation between fluctuations and efficiency at maximum power for small heat engines, *Phys. Rev. Research* **4**, 043139 (2022).
 - [14] A. Dechant, N. Kiesel, and E. Lutz, Underdamped stochastic heat engine at maximum efficiency, *Europhys. Lett.* **119**, 50003 (2017).
 - [15] Y. H. Chen, J.-F. Chen, Z. Fei, and H. T. Quan, Microscopic theory of the Curzon-Ahlborn heat engine based on a Brownian particle, *Phys. Rev. E* **106**, 024105 (2022).
 - [16] F. L. Curzon and B. Ahlborn, Efficiency of a Carnot engine at maximum power output, *Am. J. Phys.* **43**, 22 (1975).
 - [17] P. Salamon and R. S. Berry, Thermodynamic Length and Dissipated Availability, *Phys. Rev. Lett.* **51**, 1127 (1983).
 - [18] G. E. Crooks, Measuring Thermodynamic Length, *Phys. Rev. Lett.* **99**, 100602 (2007).
 - [19] D. A. Sivak and G. E. Crooks, Thermodynamic Metrics and Optimal Paths, *Phys. Rev. Lett.* **108**, 190602 (2012).
 - [20] P. R. Zulkowski, D. A. Sivak, G. E. Crooks, and M. R. DeWeese, Geometry of thermodynamic control, *Phys. Rev. E* **86**, 041148 (2012).
 - [21] M. Scandi and M. Perarnau-Llobet, Thermodynamic length in open quantum systems, *Quantum* **3**, 197 (2019).
 - [22] V. Cavina, A. Mari, and V. Giovannetti, Slow Dynamics and Thermodynamics of Open Quantum Systems, *Phys. Rev. Lett.* **119**, 050601 (2017).

- [23] K. Brandner and K. Saito, Thermodynamic Geometry of Microscopic Heat Engines, *Phys. Rev. Lett.* **124**, 040602 (2020).
- [24] J.-F. Chen, C. P. Sun, and H. Dong, Extrapolating the thermodynamic length with finite-time measurements, *Phys. Rev. E* **104**, 034117 (2021).
- [25] P. Abiuso and M. Perarnau-Llobet, Optimal Cycles for Low-Dissipation Heat Engines, *Phys. Rev. Lett.* **124**, 110606 (2020).
- [26] G. Li, J.-F. Chen, C. P. Sun, and H. Dong, Geodesic Path for the Minimal Energy Cost in Shortcuts to Isothermality, *Phys. Rev. Lett.* **128**, 230603 (2022).
- [27] J.-F. Chen, Optimizing Brownian heat engine with shortcut strategy, *Phys. Rev. E* **106**, 054108 (2022).
- [28] A. G. Frim and M. R. DeWeese, Geometric Bound on the Efficiency of Irreversible Thermodynamic Cycles, *Phys. Rev. Lett.* **128**, 230601 (2022).
- [29] Z. Wang and J. Ren, Thermodynamic Geometry of Nonequilibrium Fluctuations in Cyclically Driven Transport, (2023), 10.48550/ARXIV.2304.08181, arXiv:2304.08181 [cond-mat.stat-mech].
- [30] L. S. Pontryagin, V. G. Boltyanskii, R. V. Gamkrelidze, and E. F. Mishchenko, *The Mathematical Theory of Optimal Processes* (Wiley, New York, 1962).
- [31] A. P. Peirce, M. A. Dahleh, and H. Rabitz, Optimal control of quantum-mechanical systems: Existence, numerical approximation, and applications, *Phys. Rev. A* **37**, 4950 (1988).
- [32] T. Caneva, M. Murphy, T. Calarco, R. Fazio, S. Montangero, V. Giovannetti, and G. E. Santoro, Optimal Control at the Quantum Speed Limit, *Phys. Rev. Lett.* **103**, 240501 (2009).
- [33] S. Lloyd and S. Montangero, Information Theoretical Analysis of Quantum Optimal Control, *Phys. Rev. Lett.* **113**, 010502 (2014).
- [34] J. Li, X. Yang, X. Peng, and C.-P. Sun, Hybrid Quantum-Classical Approach to Quantum Optimal Control, *Phys. Rev. Lett.* **118**, 150503 (2017).
- [35] U. Boscain, M. Sigalotti, and D. Sugny, Introduction to the Pontryagin Maximum Principle for Quantum Optimal Control, *PRX Quantum* **2**, 030203 (2021).
- [36] Z.-C. Yang, A. Rahmani, A. Shabani, H. Neven, and C. Chamon, Optimizing Variational Quantum Algorithms Using Pontryagin's Minimum Principle, *Phys. Rev. X* **7**, 021027 (2017).
- [37] L. T. Brady, C. L. Baldwin, A. Bapat, Y. Kharkov, and A. V. Gorshkov, Optimal Protocols in Quantum Annealing and Quantum Approximate Optimization Algorithm Problems, *Phys. Rev. Lett.* **126**, 070505 (2021).
- [38] M. H. Rubin, Optimal configuration of a class of irreversible heat engines. II, *Phys. Rev. A* **19**, 1277 (1979).
- [39] V. Cavina, A. Mari, A. Carlini, and V. Giovannetti, Optimal thermodynamic control in open quantum systems, *Phys. Rev. A* **98**, 012139 (2018).
- [40] H. Kramers, Brownian motion in a field of force and the diffusion model of chemical reactions, *Physica* **7**, 284 (1940).
- [41] Y. Rezek and R. Kosloff, Irreversible performance of a quantum harmonic heat engine, *New J. Phys.* **8**, 83 (2006).
- [42] J.-F. Chen and H. T. Quan, Hierarchical structure of fluctuation theorems for a driven system in contact with multiple heat reservoirs, *Phys. Rev. E* **107**, 024135 (2023).
- [43] Supplementary Materials, SupplementaryMaterials.
- [44] Z. Gong, Y. Lan, and H. Quan, Stochastic Thermodynamics of a Particle in a Box, *Phys. Rev. Lett.* **117**, 180603 (2016).
- [45] D. S. P. Salazar, Work distribution in thermal processes, *Phys. Rev. E* **101**, 030101 (2020).
- [46] L. Mandelstam and I. G. Tamm, The uncertainty relation between energy and time in nonrelativistic quantum mechanics, *J. Phys. USSR* **9**, 249 (1945).
- [47] N. Margolus and L. B. Levitin, The maximum speed of dynamical evolution, *Phys. D: Nonlinear Phenom.* **120**, 188 (1998).
- [48] M. V. Berry, Transitionless quantum driving, *J. Phys. A: Math. Theor.* **42**, 365303 (2009).
- [49] D. Guéry-Odelin, A. Ruschhaupt, A. Kiely, E. Torrontegui, S. Martínez-Garaot, and J. G. Muga, Shortcuts to adiabaticity: Concepts, methods, and applications, *Rev. Mod. Phys.* **91**, 045001 (2019).
- [50] R. Uzdin, A. Levy, and R. Kosloff, Quantum Heat Machines Equivalence, Work Extraction beyond Markovianity, and Strong Coupling via Heat Exchangers, *Entropy* **18**, 124 (2016).
- [51] D. Gelbwaser-Klimovsky and A. Aspuru-Guzik, Strongly Coupled Quantum Heat Machines, *J. Phys. Chem. Lett.* **6**, 3477 (2015).
- [52] M. Perarnau-Llobet, H. Wilming, A. Riera, R. Gallego, and J. Eisert, Strong Coupling Corrections in Quantum Thermodynamics, *Phys. Rev. Lett.* **120**, 120602 (2018).
- [53] L. Chen and Z. Yan, The effect of heat-transfer law on performance of a two-heat-source endoreversible cycle, *J. Chem. Phys.* **90**, 3740 (1989).
- [54] N. Shiraishi, K. Saito, and H. Tasaki, Universal trade-off relation between power and efficiency for heat engines, *Phys. Rev. Lett.* **117**, 190601 (2016).
- [55] P. Pietzonka and U. Seifert, Universal trade-off between power, efficiency, and constancy in steady-state heat engines, *Phys. Rev. Lett.* **120**, 190602 (2018).
- [56] Y.-H. Ma, D. Xu, H. Dong, and C.-P. Sun, Universal constraint for efficiency and power of a low-dissipation heat engine, *Phys. Rev. E* **98**, 042112 (2018).
- [57] V. Holubec and A. Ryabov, Maximum efficiency of low-dissipation heat engines at arbitrary power, *J. Stat. Mech: Theory Exp.* **2016**, 073204 (2016).

Supplementary materials: Optimal control theory for maximum power of Brownian heat engines

Jin-Fu Chen^{1,*} and H. T. Quan^{1,2,3,†}

¹*School of Physics, Peking University, Beijing, 100871, China*

²*Collaborative Innovation Center of Quantum Matter, Beijing 100871, China*

³*Frontiers Science Center for Nano-optoelectronics, Peking University, Beijing, 100871, China*

(Dated: October 31, 2023)

CONTENTS

I. Optimization in general damped situation	1
A. Isothermal processes	2
B. Switchings: connecting processes	3
C. Construction of the optimal cycle	4
II. Optimization in underdamped limit	5
Construction of heat-engine cycles	6
III. Optimization in overdamped limit	7
Construction of heat-engine cycles	9
IV. Output power of sliced cycle	12
A. General damped situation	12
B. Overdamped limit	14
C. Underdamped limit	15
D. Maximum output power in general damped situation	15
References	15

I. OPTIMIZATION IN GENERAL DAMPED SITUATION

We start from the approximate dynamics of the potential energy

$$\dot{V} = \frac{\kappa^2 + \lambda}{\kappa^2 + 2\lambda} \alpha V - \frac{\kappa\lambda(2V - T_b)}{(\kappa^2 + 2\lambda)}. \quad (1)$$

where $\alpha = \dot{\lambda}/\lambda$ is the rate of varying the stiffness. The work rate during the isothermal process is

$$\dot{W} = \alpha V. \quad (2)$$

We want to maximize the output work

$$W_{\text{out}} = -W = \int_0^\tau \alpha V dt. \quad (3)$$

To include the evolution equations (1) and $\dot{\lambda} = \alpha\lambda$ as dynamical constraints, we introduce the Lagrange multipliers ψ_V and ψ_λ and construct the Lagrangian

* chenjinfu@pku.edu.cn

† htquan@pku.edu.cn

$$\mathcal{L} = -\alpha V + \psi_V \left[\frac{\kappa^2 + \lambda}{\kappa^2 + 2\lambda} \alpha V - \frac{\kappa\lambda(2V - T_b)}{\kappa^2 + 2\lambda} - \dot{V} \right] + \psi_\lambda(\alpha\lambda - \dot{\lambda}). \quad (4)$$

When the control parameters are varied under some constraints, it is more convenient to use the pseudo Hamiltonian [1]

$$\mathcal{H} = \psi_V \dot{V} + \psi_\lambda \dot{\lambda} + \mathcal{L} \quad (5)$$

$$= -\alpha V + \psi_V \left[\frac{\kappa^2 + \lambda}{\kappa^2 + 2\lambda} \alpha V - \frac{\kappa\lambda(2V - T_b)}{\kappa^2 + 2\lambda} \right] + \psi_\lambda \lambda \alpha, \quad (6)$$

where the state variables are V and λ , the corresponding costate variables are ψ_V and ψ_λ , and the control parameters are the rate of stiffness change α and the bath temperature T_b . The evolution of the state variables is generated by

$$\dot{V} = \frac{\partial \mathcal{H}}{\partial \psi_V} = \frac{\kappa^2 + \lambda}{\kappa^2 + 2\lambda} \alpha V - \frac{\kappa\lambda(2V - T_b)}{\kappa^2 + 2\lambda}, \quad (7)$$

$$\dot{\lambda} = \frac{\partial \mathcal{H}}{\partial \psi_\lambda} = \alpha \lambda. \quad (8)$$

The evolution of the costate variables is generated by

$$\dot{\psi}_V = -\frac{\partial \mathcal{H}}{\partial V} = \alpha \left[1 - \frac{(\kappa^2 + \lambda) \psi_V}{\kappa^2 + 2\lambda} \right] + \frac{2\kappa\lambda\psi_V}{\kappa^2 + 2\lambda}, \quad (9)$$

$$\dot{\psi}_\lambda = -\frac{\partial \mathcal{H}}{\partial \lambda} = \alpha \left[\frac{\kappa^2 V \psi_V}{(\kappa^2 + 2\lambda)^2} - \psi_\lambda \right] - \frac{\kappa^3(T_b - 2V)\psi_V}{(\kappa^2 + 2\lambda)^2}. \quad (10)$$

The control parameters are varied to possibly maximize the pseudo Hamiltonian. The control of bath temperature is determined by

$$\frac{\partial \mathcal{H}}{\partial T_b} = \frac{\kappa\lambda\psi_V}{\kappa^2 + 2\lambda}, \quad (11)$$

which corresponds to a bang-bang control $T_b = T_H$ for $\psi_V > 0$ and T_L for $\psi_V < 0$. The control of the stiffness change rate α is determined from

$$\frac{\partial \mathcal{H}}{\partial \alpha} = \lambda\psi_\lambda + \frac{V(\kappa^2 + \lambda)\psi_V}{\kappa^2 + 2\lambda} - V, \quad (12)$$

which does not depend on α .

A. Isothermal processes

We first consider the singular control with $\partial \mathcal{H} / \partial \alpha = 0$. We eliminate ψ_V and ψ_λ from Eq. (12) as

$$\psi_V = \frac{(\kappa^2 + 2\lambda)(T_b - 2V)}{\lambda T_b + 2\kappa^2 V}, \quad (13)$$

$$\psi_\lambda = \frac{V[2V(2\kappa^2 + \lambda) - \kappa^2 T_b]}{\lambda(\lambda T_b + 2\kappa^2 V)}, \quad (14)$$

and obtain the solution to the control parameter

$$\alpha = \frac{\kappa\lambda(2V - T_b)[2\kappa^2 V + (\kappa^2 + 2\lambda)T_b]}{V[4\kappa^4 V + 6\kappa^2 \lambda V + (\kappa^2 + 2\lambda)\lambda T_b]}. \quad (15)$$

The conserved pseudo Hamiltonian is obtained

$$\mathcal{H} = \frac{\kappa\lambda(T_b - 2V)^2}{\lambda T_b + 2\kappa^2 V}. \quad (16)$$

We can solve the stiffness as

$$\lambda = \frac{2\kappa^2 V \mathcal{H}}{\kappa(T_b - 2V)^2 - T_b \mathcal{H}}. \quad (17)$$

Substituting Eq. (15) into Eqs. (7) and (8), we obtain

$$\dot{V} = -\frac{\kappa^3 \lambda (T_b - 2V)^2}{2\lambda^2 T_b + \kappa^2 \lambda (T_b + 6V) + 4\kappa^4 V}, \quad (18)$$

$$\dot{\lambda} = \frac{\kappa\lambda^2(2V - T_b) [2\kappa^2 V + T_b(\kappa^2 + 2\lambda)]}{V [4\kappa^4 V + 6\kappa^2 \lambda V + T_b(\kappa^2 + 2\lambda)\lambda]}. \quad (19)$$

We determine the work in the isothermal process as

$$W_{\text{iso}} = \int_{\lambda_i}^{\lambda_f} V \frac{d\lambda}{\lambda} \quad (20)$$

$$= \int_{V_i}^{V_f} \frac{\kappa T_b^2 - \mathcal{H} T_b - 4\kappa V^2}{\kappa(T_b - 2V)^2 - \mathcal{H} T_b} dV \quad (21)$$

$$= \left[-\frac{1}{2} T_b \ln(\kappa(T_b - 2V)^2 - \mathcal{H} T_b) - \sqrt{\frac{\mathcal{H} T_b}{\kappa}} \tanh^{-1} \left(\sqrt{\frac{\kappa}{\mathcal{H} T_b}} (T_b - 2V) \right) - V \right] \Big|_{V=V_i}^{V_f}. \quad (22)$$

The operation time of the isothermal process is

$$\tau_{\text{iso}} = \int_{V_i}^{V_f} \frac{dV}{\dot{V}} \quad (23)$$

$$= - \int_{V_i}^{V_f} \frac{2\kappa^2 (T_b - 2V)^3 - 3\kappa\mathcal{H} (T_b - 2V)^2 + \mathcal{H}^2 T_b}{\kappa\mathcal{H} (T_b - 2V) (\kappa(T_b - 2V)^2 - \mathcal{H} T_b)} dV \quad (24)$$

$$= \left[-\frac{\ln(\kappa(T_b - 2V)^2 - \mathcal{H} T_b)}{2\kappa} - \frac{\ln(2V - T_b)}{2\kappa} - \sqrt{\frac{T_b}{\kappa\mathcal{H}}} \tanh^{-1} \left(\sqrt{\frac{\kappa}{\mathcal{H} T_b}} (T_b - 2V) \right) - \frac{2V}{\mathcal{H}} \right] \Big|_{V=V_i}^{V_f}. \quad (25)$$

B. Switchings: connecting processes

To construct cycles, we need to find some switchings to connect the two singular isothermal processes at temperatures $T_b = T_L$ and T_H . The switchings can be realized by simultaneously changing T_b and λ instantaneously, where the heat exchanged can be neglected. Therefore, the evolution of the state variables and costate variables during the switchings is reduced to

$$\dot{V} = \frac{\kappa^2 + \lambda}{\kappa^2 + 2\lambda} \alpha V, \quad (26)$$

$$\dot{\lambda} = \alpha \lambda, \quad (27)$$

$$\dot{\psi}_V = \alpha \left[1 - \frac{(\kappa^2 + \lambda) \psi_V}{\kappa^2 + 2\lambda} \right], \quad (28)$$

$$\dot{\psi}_\lambda = \alpha \left[\frac{\kappa^2 V \psi_V}{(\kappa^2 + 2\lambda)^2} - \psi_\lambda \right]. \quad (29)$$

Thus the values of the potential energy V and its costate variable ψ_V at the beginning and the end of the switchings should satisfy

$$\frac{V_f \sqrt{\kappa^2 + 2\lambda_f}}{\lambda_i} = \frac{V_i \sqrt{2\lambda_i + \kappa^2}}{\lambda_i}, \quad (30)$$

$$\frac{\lambda_f(\psi_{V_f} - 2) - \kappa^2}{\sqrt{\kappa^2 + 2\lambda_f}} = \frac{\lambda_i(\psi_{V_i} - 2) - \kappa^2}{\sqrt{\kappa^2 + 2\lambda_i}}. \quad (31)$$

We calculate the work of the connecting process as

$$W_{\text{con}} = \int_{\lambda_i}^{\lambda_f} \frac{d\lambda}{\lambda} V \quad (32)$$

$$= \frac{V_i}{\lambda_i} \sqrt{\kappa^2 + 2\lambda_i} \int_{\lambda_i}^{\lambda_f} \frac{d\lambda}{\sqrt{\kappa^2 + 2\lambda}} \quad (33)$$

$$= \frac{V_i}{\lambda_i} \sqrt{\kappa^2 + 2\lambda_i} (\sqrt{\kappa^2 + 2\lambda_f} - \sqrt{\kappa^2 + 2\lambda_i}). \quad (34)$$

Notice that the pseudo Hamiltonian \mathcal{H} should be conserved in the optimal control of the whole cycle. We will use the conservation of \mathcal{H} to determine the switching.

C. Construction of the optimal cycle

Using the conservation of \mathcal{H} and the control constraints of the stiffness $\lambda_L \leq \lambda \leq \lambda_H$, we find two switchings that can be realized by using the lower and the upper stiffness constraints λ_L and λ_H respectively. We first consider the switching by increasing λ to λ_H . This happens during the cold isothermal process by simultaneously changing the stiffness from λ_2 to λ_H and the bath temperature from T_L to T_H . The conservation of \mathcal{H} leads to

$$\mathcal{H} = \frac{\kappa\lambda(T_L - 2V_2)^2}{\lambda T_L + 2\kappa^2 V_2} = -\psi_{V_3} \frac{\kappa\lambda_H(2V_3 - T_H)}{\kappa^2 + 2\lambda_H}, \quad (35)$$

where ψ_{V_3} is given by Eq. (13). We solve this connecting process by using the fact that V_3 and ψ_{V_3} are related to V_2 and ψ_{V_2} according to Eqs. (30) and (31).

Similarly, the other switching by decreasing λ to λ_L happens during the hot isothermal process by simultaneously changing the stiffness from λ_5 to λ_L and the bath temperature from T_H to T_L . The conservation of \mathcal{H} leads to

$$\mathcal{H} = \frac{\kappa\lambda_5(T_H - 2V_5)^2}{\lambda_5 T_H + 2\kappa^2 V_5} = -\psi_{V_6} \frac{\kappa\lambda_L(2V_6 - T_L)}{\kappa^2 + 2\lambda_L}. \quad (36)$$

Given specific λ_L , we identify the maximum \mathcal{H} such that point 6 approaches to point 1 on the cold isothermal curve. When \mathcal{H} is larger than the maximum value, the lower switching connects the two isothermal processes directly without reaching λ_L .

We determine the maximum \mathcal{H} from the conservation of pseudo Hamiltonian

$$\mathcal{H} = \frac{\kappa\lambda_5(T_H - 2V_5)^2}{\lambda_5 T_H + 2\kappa^2 V_5} = \frac{\kappa\lambda_L(T_L - 2V_1)^2}{\lambda_L T_L + 2\kappa^2 V_1}. \quad (37)$$

Points 1 and 5 are on the cold and the hot isothermal curves respectively, and they satisfy the relation of the switching

$$\frac{V_1}{\lambda_L} \sqrt{\kappa^2 + 2\lambda_L} = \frac{V_5}{\lambda_5} \sqrt{\kappa^2 + 2\lambda_5}, \quad (38)$$

$$\frac{\lambda_L(\psi_{V_1} - 2) - \kappa^2}{\sqrt{\kappa^2 + 2\lambda_L}} = \frac{\lambda_5(\psi_{V_5} - 2) - \kappa^2}{\sqrt{\kappa^2 + 2\lambda_5}}, \quad (39)$$

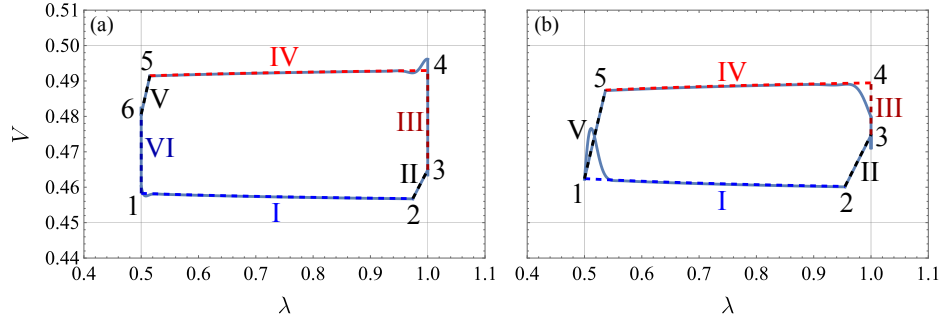


Figure 1. Diagrams of heat-engine cycles. (a) $\mathcal{H} = 10^{-4}$ (non-maximum- \mathcal{H}) and (b) $\mathcal{H} = 2.246 \times 10^{-4}$ (maximum- \mathcal{H}). The friction coefficient is $\kappa = 1$, and the control constraints $T_L = 0.9$, $T_H = 1$, $\lambda_L = 0.5$ and $\lambda_H = 1$ are depicted by the horizontal and vertical gray lines. The dashed curves represent the estimated evolution, while the solid curves are the exact evolution for the limit cycles.

and ψ_{V_1} and ψ_{V_5} are related to V_1 and V_5 according to Eq. (13). Thus the maximum \mathcal{H} is determined by λ_L , T_L and T_H , but we only obtain the numerical results in general damped situation. We will show analytical results of the maximum \mathcal{H} in the underdamped and the overdamped limits in Sec. II and Sec. III, respectively. The output power of the maximum- \mathcal{H} cycle is

$$P = -\frac{W_I + W_{II} + W_{IV} + W_V}{\tau_I + \tau_{III} + \tau_{IV}}, \quad (40)$$

where we evaluate the work W_I and W_{IV} of two isothermal processes by Eq. (22), the work W_{II} and W_V of the two connecting processes by Eq. (34), the duration τ_I and τ_{IV} of two isothermal processes by Eq. (25), the duration of the isochoric relaxation by

$$\tau_{III} = \frac{\kappa^2 + 2\lambda}{\kappa\lambda} \ln \frac{2V_3 - T_H}{2V_4 - T_H}. \quad (41)$$

As an illustration, we show cycle diagrams λ - V in Fig. 1 under the parameters $T_L = 0.9$, $T_H = 1$, $\lambda_L = 0.5$, $\lambda_H = 1$, and $\kappa = 1$. The control of a whole cycle is determined by \mathcal{H} . Increasing the output power is converted to finding the cycle with larger \mathcal{H} . For larger \mathcal{H} , the path of the process VI becomes shorter. For the maximum \mathcal{H} , process VI diminishes and point 6 approaches to point 1, as shown in Fig. 1(b). In the following, we focus on maximum- \mathcal{H} cycles for given control constraints. To improve the output power, we need to construct the maximum- \mathcal{H} cycles with appropriate friction coefficient κ .

II. OPTIMIZATION IN UNDERDAMPED LIMIT

We discuss the optimization of the cycle in the underdamped limit $\kappa^2 \ll \lambda$. The pseudo Hamiltonian (6) becomes

$$\mathcal{H} = -\alpha V + \psi_V \left[\frac{1}{2}\alpha V - \kappa \left(V - \frac{T_b}{2} \right) \right] + \psi_\lambda \lambda \alpha. \quad (42)$$

The evolution of the state variables and costate variables is given by

$$\dot{V} = \frac{\partial \mathcal{H}}{\partial \psi_V} = \frac{1}{2}\alpha V - \kappa \left(V - \frac{T_b}{2} \right), \quad (43)$$

$$\dot{\lambda} = \frac{\partial \mathcal{H}}{\partial \psi_\lambda} = \alpha \lambda, \quad (44)$$

$$\dot{\psi}_V = -\frac{\partial \mathcal{H}}{\partial V} = \alpha - \psi_V \left(\frac{\alpha}{2} - \kappa \right), \quad (45)$$

$$\dot{\psi}_\lambda = -\frac{\partial \mathcal{H}}{\partial \lambda} = -\alpha \psi_\lambda. \quad (46)$$

The control of bath temperature is determined by

$$\frac{\partial \mathcal{H}}{\partial T_b} = \frac{\kappa \psi_V}{2}, \quad (47)$$

which corresponds to a bang-bang control $T_b = T_H$ for $\psi_V > 0$ and T_L for $\psi_V < 0$. The control of the stiffness change rate α is determined from

$$\frac{\partial \mathcal{H}}{\partial \alpha} = \psi_\lambda \lambda + \left(\frac{\psi_V}{2} - 1\right)V. \quad (48)$$

Similarly, the singular control is given by $\partial \mathcal{H} / \partial \alpha = 0$, and we eliminate ψ_V and ψ_λ as

$$\psi_V = 2 - \frac{4V}{T_b}, \quad (49)$$

$$\psi_\lambda = \frac{2V^2}{\lambda T_b}. \quad (50)$$

The singular optimal control is given by

$$\alpha = \kappa \left(2 - \frac{T_b}{V}\right). \quad (51)$$

Together with the evolution equation (43), we find that in the singular control $\dot{V} = 0$, and therefore $\dot{\lambda} / \lambda = \alpha$ remains constant. Such exponential protocols have been found as the optimal protocols in the underdamped limit [2–5]. Substituting Eqs. (49) and (50) into Eq. (42), the pseudo Hamiltonian is explicitly

$$\mathcal{H} = \frac{\kappa (T_b - 2V)^2}{T_b}, \quad (52)$$

which is consistent with Eq. (16) by taking the underdamped limit $\kappa^2 \ll \lambda$. From Eq. (52), we obtain the potential energy is constant in the singular control

$$V = \frac{1}{2} \left(T_b \pm \sqrt{\frac{T_b \mathcal{H}}{\kappa}}\right). \quad (53)$$

We next consider the switchings between the two isothermal curves $T_b = T_L$ and T_H , and construct the maximum- \mathcal{H} cycle in the underdamped limit.

Construction of heat-engine cycles

It is similar to construct heat-engine cycles according to Subsection IC. The maximum- \mathcal{H} cycle is determined by

$$\mathcal{H} = \frac{\kappa (T_H - 2V_5)^2}{T_H} = \frac{\kappa (T_L - 2V_1)^2}{T_L}. \quad (54)$$

Points 1 and 5 are on the cold and the hot isothermal curves respectively, and they satisfy the relation of the switching

$$\frac{V_1}{\sqrt{\lambda_L}} = \frac{V_5}{\sqrt{\lambda_5}}, \quad (55)$$

$$\sqrt{\lambda_L}(\psi_{V1} - 2) = \sqrt{\lambda_5}(\psi_{V5} - 2). \quad (56)$$

We obtain the solution

$$V_1 = \frac{1}{4}(T_L + \sqrt{T_H T_L}), \quad (57)$$

$$V_5 = \frac{1}{4}(T_H + \sqrt{T_H T_L}), \quad (58)$$

$$\mathcal{H} = \frac{\kappa}{4}(\sqrt{T_H} - \sqrt{T_L})^2. \quad (59)$$

And the rate of the stiffness change is

$$\alpha = \begin{cases} 2\kappa \frac{\sqrt{T_H} - \sqrt{T_L}}{\sqrt{T_H} + \sqrt{T_L}}, & T_b = T_L \\ -2\kappa \frac{\sqrt{T_H} - \sqrt{T_L}}{\sqrt{T_H} + \sqrt{T_L}}, & T_b = T_H \end{cases} \quad (60)$$

Since V remains constant in the singular control in the underdamped limit, we obtain $V_2 = V_1$ and $V_4 = V_5$, and the isochoric process III also diminishes in the maximum- \mathcal{H} cycle, i.e., $V_3 = V_5$.

The work and the operation time of each process in the underdamped limit can be easily calculated. Here we just list the results in the following. The performed work of each process is

$$W_I = V_1 \ln \frac{\lambda_2}{\lambda_L} = \frac{1}{4}(T_L + \sqrt{T_H T_L}) \ln \frac{\lambda_2}{\lambda_L}, \quad (61)$$

$$W_{II} = 2V_3 - 2V_2 = \frac{1}{2}(T_H - T_L), \quad (62)$$

$$W_{IV} = V_4 \ln \frac{\lambda_5}{\lambda_H} = -\frac{1}{4}(T_H + \sqrt{T_H T_L}) \ln \frac{\lambda_2}{\lambda_L}, \quad (63)$$

$$W_V = 2V_1 - 2V_5 = -\frac{1}{2}(T_H - T_L), \quad (64)$$

and the operation time is

$$\tau_I = \tau_{IV} = \frac{\sqrt{T_H} + \sqrt{T_L}}{2\kappa(\sqrt{T_H} - \sqrt{T_L})} \ln \frac{\lambda_2}{\lambda_L}, \quad (65)$$

$$\tau_{III} = 0. \quad (66)$$

According to Eq. (40), we obtain the maximum output power in the underdamped limit [3, 5]

$$P_{\text{under}}^* = \frac{\kappa}{4}(\sqrt{T_H} - \sqrt{T_L})^2. \quad (67)$$

which does not depend on the stiffness constraints, since the system is scaled invariant in the underdamped limit.

III. OPTIMIZATION IN OVERDAMPED LIMIT

We discuss the optimization of the cycle in the overdamped limit $\kappa^2 \gg \lambda$. The pseudo Hamiltonian (6) becomes

$$\mathcal{H} = -\alpha V + \psi_V \left[\alpha V - \frac{\lambda(2V - T_b)}{\kappa} \right] + \psi_\lambda \lambda \alpha. \quad (68)$$

The evolution of the state variables and costate variables is given by

$$\dot{V} = \frac{\partial \mathcal{H}}{\partial \psi_V} = \alpha V - \frac{\lambda(2V - T_b)}{\kappa}, \quad (69)$$

$$\dot{\lambda} = \frac{\partial \mathcal{H}}{\partial \psi_\lambda} = \alpha \lambda, \quad (70)$$

$$\dot{\psi}_V = -\frac{\partial \mathcal{H}}{\partial V} = \psi_V \left(\frac{2\lambda}{\kappa} - \alpha \right) + \alpha, \quad (71)$$

$$\dot{\psi}_\lambda = -\frac{\partial \mathcal{H}}{\partial \lambda} = -\frac{\alpha \kappa \psi_\lambda + \psi_V (T_b - 2V)}{\kappa}. \quad (72)$$

The control of bath temperature is determined by

$$\frac{\partial \mathcal{H}}{\partial T_b} = \frac{\lambda}{\kappa} \psi_V, \quad (73)$$

which corresponds to a bang-bang control $T_b = T_H$ for $\psi_V > 0$ and T_L for $\psi_V < 0$. The control of the stiffness change rate α is determined from

$$\frac{\partial \mathcal{H}}{\partial \alpha} = \lambda \psi_\lambda + V (\psi_V - 1). \quad (74)$$

The singular control is given by $\partial \mathcal{H} / \partial \alpha = 0$. We eliminate the costate variables

$$\psi_V = \frac{T_b}{2V} - 1, \quad (75)$$

$$\psi_\lambda = \frac{2V}{\lambda} - \frac{T_b}{2\lambda}, \quad (76)$$

and obtain the singular optimal control as

$$\alpha = \frac{\lambda}{\kappa} \left(1 - \frac{T_b^2}{4V^2} \right). \quad (77)$$

The differential equations for the optimal control are

$$\dot{\lambda} = \frac{\lambda^2}{\kappa} \left(1 - \frac{T_b^2}{4V^2} \right), \quad (78)$$

$$\dot{V} = -\frac{\lambda}{\kappa V} \left(V - \frac{T_b}{2} \right)^2. \quad (79)$$

Under the initial condition $\lambda(0) = \lambda_0$ and $V(0) = V_0$, we obtain the solution

$$V(t) = V_0 - \frac{\lambda_0 t (T_b - 2V_0)^2}{4\kappa V_0}, \quad (80)$$

$$\lambda(t) = \frac{\kappa \lambda_0 [4\kappa V_0^2 - \lambda_0 t (T_b - 2V_0)^2]}{[\lambda_0 t (T_b - 2V_0) + 2\kappa V_0]^2}. \quad (81)$$

which coincides with the control scheme obtained in Refs. [6, 7].

Substituting Eqs. (75) and (76) into Eq. (68), the pseudo Hamiltonian is explicitly

$$\mathcal{H} = \frac{\lambda (T_b - 2V)^2}{2\kappa V}. \quad (82)$$

This expression is consistent with Eq. (16) by taking the overdamped limit $\kappa^2 \gg \lambda$. Therefore, the potential energy is related to the stiffness as

$$V = \frac{T_b}{2} + \frac{\kappa \mathcal{H}}{4\lambda} \left(1 \pm \sqrt{\frac{4\lambda T_b}{\kappa \mathcal{H}} + 1} \right). \quad (83)$$

The work in an isothermal process can be obtained as

$$W_{\text{iso}}^{\text{over}} = \int_{\lambda_i}^{\lambda_f} \frac{V}{\lambda} d\lambda \quad (84)$$

$$= \int_{V_i}^{V_f} \frac{T_b + 2V}{T_b - 2V} dV \quad (85)$$

$$= V_i - V_f + T_b \ln \frac{2V_i - T_b}{2V_f - T_b}. \quad (86)$$

The operation time is

$$\tau_{\text{iso}}^{\text{over}} = \int_{V_i}^{V_f} \frac{dV}{\dot{V}} \quad (87)$$

$$= - \int_{V_i}^{V_f} \frac{4\kappa V}{\lambda (2V - T_b)^2} dV \quad (88)$$

$$= 2 \frac{V_i - V_f}{\mathcal{H}}. \quad (89)$$

Thus, we obtain the work and operation time for processes I and IV in the overdamped limit.

Construction of heat-engine cycles

In the switchings, the stiffness is rapidly changed and the heat exchange can be neglected. The differential equations (69)-(72) of the state variables and costate variables are reduced to

$$\dot{V} = \alpha V, \quad (90)$$

$$\dot{\lambda} = \alpha \lambda, \quad (91)$$

$$\dot{\psi}_V = (1 - \psi_V) \alpha, \quad (92)$$

$$\dot{\psi}_\lambda = -\alpha \psi_\lambda. \quad (93)$$

The work in these connecting processes is obtained as

$$W_{\text{con}}^{\text{over}} = V_f - V_i. \quad (94)$$

When the stiffness is switched to λ_H , an isochoric relaxation process follows

$$\dot{V} = - \frac{\lambda_H (2V - T_H)}{\kappa}, \quad (95)$$

$$\dot{\lambda} = 0, \quad (96)$$

$$\dot{\psi}_V = \psi_V \frac{2\lambda_H}{\kappa}, \quad (97)$$

$$\dot{\psi}_\lambda = - \frac{\psi_V (T_H - 2V)}{\kappa}. \quad (98)$$

We first calculate the left switching of the maximum- \mathcal{H} cycle in the overdamped limit. The two boundary points 1 and 5 satisfy

$$\frac{V_5}{\lambda_5} = \frac{V_1}{\lambda_L}, \quad (99)$$

$$(1 - \psi_{V_5}) \lambda_5 = (1 - \psi_{V_1}) \lambda_L, \quad (100)$$

where ψ_{V_1} and ψ_{V_5} are related to V_1 and V_5 by Eq. (75). The two points locate on two isothermal curves, and the conservation of \mathcal{H} leads to

$$\mathcal{H} = \frac{\lambda_L (T_L - 2V_1)^2}{2\kappa V_1} = \frac{\lambda_5 (T_H - 2V_5)^2}{2\kappa V_5}. \quad (101)$$

From Eqs. (99)-(101), we obtain the solution of the left switching for the maximum- \mathcal{H} cycle

$$\mathcal{H} = \frac{(T_H - T_L)^2 \lambda_L}{4(T_H + 3T_L)\kappa}, \quad (102)$$

$$V_1 = \frac{1}{8}(T_H + 3T_L), \quad (103)$$

$$\psi_{V1} = -\frac{T_H - T_L}{T_H + 3T_L}, \quad (104)$$

$$\lambda_5 = \frac{3T_H + T_L}{T_H + 3T_L} \lambda_L, \quad (105)$$

$$V_5 = \frac{1}{8}(3T_H + T_L), \quad (106)$$

$$\psi_{V5} = \frac{T_H - T_L}{3T_H + T_L}. \quad (107)$$

To achieve large \mathcal{H} , we can possibly choose large λ_L , but λ_5 should be less than λ_H , which gives

$$\lambda_L \leq \frac{T_H + 3T_L}{3T_H + T_L} \lambda_H, \quad (108)$$

and the pseudo Hamiltonian is less than

$$\mathcal{H} \leq \frac{(T_H - T_L)^2 \lambda_H}{4(3T_H + T_L)\kappa}. \quad (109)$$

We next solve the right switching with given \mathcal{H} . The potential energy and the stiffness for the points 2 and 3 satisfy

$$\mathcal{H} = \frac{\lambda_2 (T_L - 2V_2)^2}{2\kappa V_2} = -\psi_{V3} \frac{\lambda_H}{\kappa} (2V_3 - T_H), \quad (110)$$

$$\frac{V_3}{\lambda_H} = \frac{V_2}{\lambda_2}, \quad (111)$$

$$(1 - \psi_{V3})\lambda_H = (1 - \psi_{V2})\lambda_2, \quad (112)$$

$$\psi_{V2} = \frac{T_L}{2V_2} - 1. \quad (113)$$

We eliminate V_3 and ψ_{V3} and obtain

$$\mathcal{H} = \left[\left(2 - \frac{T_L}{2V_2}\right) \frac{\lambda_2}{\lambda_H} - 1 \right] \frac{\lambda_H}{\kappa} \left(2 \frac{\lambda_H V_2}{\lambda_2} - T_H\right), \quad (114)$$

$$V_2 = \frac{T_L}{2} + \frac{\kappa \mathcal{H}}{4\lambda_2} \left(1 - \sqrt{\frac{4\lambda T_L}{\kappa \mathcal{H}} + 1}\right). \quad (115)$$

We do not find simple algebra expressions of V_2 and λ_2 . However, Eqs. (114) and (115) have real solutions only when \mathcal{H} is less than a maximum value $\mathcal{H}_{\max}^{\text{over}}$. To evaluate $\mathcal{H}_{\max}^{\text{over}}$, we first eliminate λ_2 and obtain the solution $V_2 = T_H \chi$, where $\chi > T_L/(2T_H)$ is the root of a fourth-order polynomial

$$f(\chi, \frac{\kappa \mathcal{H}}{\lambda_H T_H}) = 0, \quad (116)$$

where the polynomial is explicitly

$$f(\chi, \phi) = \phi^2 ((\theta - 4\chi) - (\theta - 2\chi)^2) + \phi (\theta - 2\chi)^2 (1 - \theta + 4\chi) - (\theta - 2\chi)^4. \quad (117)$$

We use $\theta = T_L/T_H$ to denote the temperature ratio. If the polynomial has a real root satisfying $\chi > T_L/(2T_H)$, the maximum value $f(\chi^*, \phi)$ on $\chi > T_L/(2T_H)$ should be positive. Thus, the maximum point satisfies

$$f(\chi^*, \phi) \geq 0, \quad (118)$$

$$\left. \frac{\partial f}{\partial \chi} \right|_{\chi=\chi^*} = 0. \quad (119)$$

Then we solve the above formulas with the equality, and obtain $\phi(\theta)$ as a positive root of a third-order polynomial

$$\phi^3 + (11 - 3\theta)\phi^2 + (3\theta^2 + 14\theta - 1)\phi - (1 - \theta)^2\theta = 0. \quad (120)$$

The positive root is explicitly

$$\phi(\theta) = \frac{1}{3} \sqrt[3]{\Upsilon(\theta)} + \frac{4}{3} \frac{(31 - 27\theta)}{\sqrt[3]{\Upsilon(\theta)}} + \theta - \frac{11}{3}, \quad (121)$$

where

$$\Upsilon(\theta) = -\frac{729\theta^2}{2} + 1809\theta - \frac{2761}{2} + \frac{3}{2}i\sqrt{3(1-\theta)(27\theta+5)^3}. \quad (122)$$

The maximum value $\mathcal{H}_{\text{over}}^{\max}$ is represented as

$$\mathcal{H}_{\text{over}}^{\max} = \frac{\lambda_H T_H}{\kappa} \phi\left(\frac{T_L}{T_H}\right). \quad (123)$$

According to Eqs. (86) and (94), we obtain the expression of the performed work for each process as

$$W_{\text{I}} = V_1 - V_2 + T_L \ln \frac{2V_1 - T_L}{2V_2 - T_L}, \quad (124)$$

$$W_{\text{II}} = V_3 - V_2, \quad (125)$$

$$W_{\text{IV}} = V_4 - V_5 + T_H \ln \frac{2V_4 - T_H}{2V_5 - T_H}, \quad (126)$$

$$W_{\text{V}} = V_1 - V_5, \quad (127)$$

and the operation time according to Eq. (89) is

$$\tau_{\text{I}} = \frac{2(V_1 - V_2)}{\mathcal{H}}, \quad (128)$$

$$\tau_{\text{III}} = \frac{\kappa}{2\lambda_H} \ln \frac{2V_3 - T_H}{2V_4 - T_H}, \quad (129)$$

$$\tau_{\text{IV}} = \frac{2(V_4 - V_5)}{\mathcal{H}}. \quad (130)$$

The output power of the maximum- \mathcal{H} cycle according to Eq. (40) is

$$P_{\text{over}} = -\frac{2V_1 - 2V_2 + V_3 + V_4 - 2V_5 + T_L \ln \frac{2V_1 - T_L}{2V_2 - T_L} + T_H \ln \frac{2V_4 - T_H}{2V_5 - T_H}}{\frac{8}{\lambda_L} \frac{(T_H + 3T_L)}{(T_H - T_L)^2} (V_1 - V_2 + V_4 - V_5) + \frac{1}{2\lambda_H} \ln \frac{2V_3 - T_H}{2V_4 - T_H}} \times \frac{1}{\kappa}. \quad (131)$$

We notice that the potential energies V_j of the maximum- \mathcal{H} cycle are solved previously by Eqs. (103), (106), and (110)-(113), and are independent of the friction coefficient κ . Therefore, we conclude the maximum output power (131) in the overdamped regime is inversely proportional to κ .

To obtain the maximum power in the overdamped limit, we consider the sliced cycle constructing around the above two switchings. This follows from a simple argument that one can always divide a cycle into several slices, and some

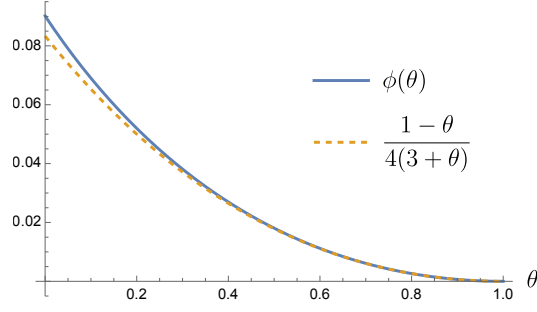


Figure 2. Comparison of Eqs. (132) and (133).

slice has the largest power among all slices. For the sliced cycles, the output power is equal to the pseudo Hamiltonian. We will show this in Sec. IV. The approximate and precise results Eqs. (109) and (120) of the maximum pseudo Hamiltonians lead to the maximum output power

$$P_{\text{over}}^{I*} = \frac{(T_H - T_L)^2 \lambda_H}{4(3T_H + T_L)\kappa}, \quad (132)$$

and

$$P_{\text{over}}^* = \frac{\lambda_H T_H}{\kappa} \phi\left(\frac{T_L}{T_H}\right), \quad (133)$$

where $\phi(\theta)$ is the root of Eq. (120). We compare the two results Eqs. (132) and (133) in Fig. 2.

IV. OUTPUT POWER OF SLICED CYCLE

A. General damped situation

We next consider the sliced cycles in the general damped situation. The diagram of a sliced cycle is shown in Fig. 3. Since the operation time of two relaxation processes is short enough, we can neglect the change of the stiffness during the two processes and just consider them as isochoric processes. Thus the cycle becomes an Otto cycle.

We consider the potential energy of point 4 is related to that of point 3 as

$$V_4 = V_3 + dV_3. \quad (134)$$

According to the switchings, we obtain the potential energy at points 2 and 6 as

$$\frac{V_2}{\lambda_2} \sqrt{\kappa^2 + 2\lambda_2} = \frac{V_3}{\lambda_H} \sqrt{\kappa^2 + 2\lambda_H}, \quad (135)$$

$$\frac{V_6}{\lambda_2} \sqrt{\kappa^2 + 2\lambda_2} = \frac{V_4}{\lambda_H} \sqrt{\kappa^2 + 2\lambda_H}. \quad (136)$$

The work in the connecting processes is

$$W_{\text{II}} = (\sqrt{\kappa^2 + 2\lambda_H} - \sqrt{\kappa^2 + 2\lambda_2}) \frac{V_3}{\lambda_H} \sqrt{\kappa^2 + 2\lambda_H}, \quad (137)$$

$$W_{\text{V}} = (\sqrt{\kappa^2 + 2\lambda_2} - \sqrt{\kappa^2 + 2\lambda_H}) \frac{V_4}{\lambda_H} \sqrt{\kappa^2 + 2\lambda_H}. \quad (138)$$

The operation time of the isochoric processes is

$$\tau_{\text{III}} = \frac{\kappa^2 + 2\lambda_H}{2\kappa\lambda_H} \ln \frac{T_H - 2V_3}{T_H - 2V_4} \quad (139)$$

$$= \frac{\kappa^2 + 2\lambda_H}{\kappa\lambda_H} \frac{dV_3}{T_H - 2V_3}, \quad (140)$$

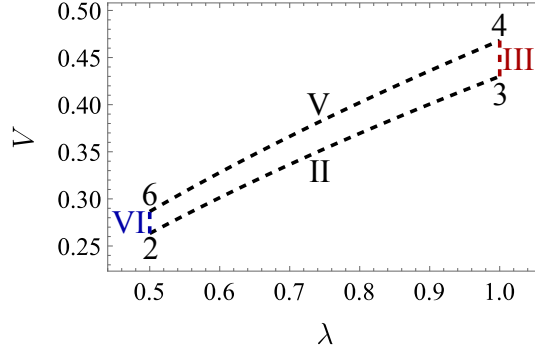


Figure 3. Diagram of a sliced cycle. It is an Otto cycle consisting of two adiabatic processes and two isochoric relaxation processes.

and

$$\tau_{VI} = \frac{\kappa^2 + 2\lambda_2}{2\kappa\lambda_2} \ln \frac{2V_6 - T_L}{2V_2 - T_L} \quad (141)$$

$$= \frac{\kappa^2 + 2\lambda_2}{\kappa\lambda_2} \frac{dV_2}{2V_2 - T_L}. \quad (142)$$

The output power is

$$P^{\text{slice}} = -\frac{W_{II} + W_V}{\tau_{III} + \tau_{VI}} \quad (143)$$

$$= \sqrt{\lambda_H} T_H \frac{\frac{\kappa}{\sqrt{\lambda_H}} (1 - \sqrt{\frac{\kappa^2 + 2\lambda_2}{\kappa^2 + 2\lambda_H}})}{\frac{T_H}{T_H - 2V_3} + \frac{\kappa^2 + 2\lambda_2}{\kappa^2 + 2\lambda_H} \frac{T_H}{2V_3 \frac{\lambda_2}{\lambda_H} - T_L \sqrt{\frac{\kappa^2 + 2\lambda_2}{\kappa^2 + 2\lambda_H}}}}. \quad (144)$$

Let us define some dimensionless quantities

$$u = \frac{\kappa}{\sqrt{\lambda_H}}, \quad (145)$$

$$y = \frac{\lambda_2}{\lambda_H}, \quad (146)$$

$$z = \frac{2V_3}{T_H}, \quad (147)$$

$$v = \sqrt{\frac{u^2 + 2y}{u^2 + 2}}. \quad (148)$$

Then we rewrite the output power as

$$P^{\text{slice}} = \sqrt{\lambda_H} T_H h(z, v, y), \quad (149)$$

where we have defined a function

$$h(z, v, y) \equiv \frac{(1-v)}{\frac{1}{1-z} + \frac{v^2}{zy - \theta v}} \sqrt{\frac{2(v^2 - y)}{1 - v^2}}. \quad (150)$$

We optimize the function $h(z, v, y)$ under the constraints $v\theta/z < y < v^2 < 1$, $0 < z < 1$ to obtain a bound on the output power. We first choose the optimal

$$z^* = \frac{v(\theta + \sqrt{y})}{v\sqrt{y} + y}, \quad (151)$$

and we obtain

$$h(z^*, v, y) = \frac{\sqrt{2}(1-v)(y-\theta v)}{(v+\sqrt{y})^2} \sqrt{\frac{v^2-y}{1-v^2}}. \quad (152)$$

We find that the bound h_{bound} can be represented as the root x of

$$\begin{aligned} & 729(\theta+1)^2 x^{12} - 108(\theta^4 + 690\theta^3 + 7893\theta^2 + 12888\theta + 5940) x^{10} \\ & + 4(\theta^6 + 2610\theta^5 + 574425\theta^4 - 3453408\theta^3 - 148824\theta^2 - 2259360\theta - 1219536) x^8 \\ & - 128(3\theta^7 + 2131\theta^6 + 85745\theta^5 - 385087\theta^4 + 983572\theta^3 - 81252\theta^2 + 48816\theta + 11880) x^6 \\ & + 512(19\theta^8 + 1288\theta^7 + 31966\theta^6 - 82560\theta^5 - 157805\theta^4 - 46328\theta^3 + 11892\theta^2 - 16\theta + 8) x^4 \\ & - 8192\theta^2(3\theta^7 + 39\theta^6 + 1294\theta^5 + 3180\theta^4 + 2883\theta^3 + 811\theta^2 - 20\theta + 2) x^2 + 16384(\theta-1)^4 \theta^4 (\theta+1)^2 = 0, \end{aligned} \quad (153)$$

where v^* and y^* are solved from

$$-2\theta v^2 + v\sqrt{y}(\theta-2v) + 2vy + y^{3/2} = 0, \quad (154)$$

$$\theta v^3 - 2(v^2-1)y^{3/2} + 2\theta v(v^2-1)\sqrt{y} + y(\theta+v^3-(\theta+1)v^2-(\theta+1)v) + y^2 = 0. \quad (155)$$

The bound on the output power is expressed by

$$P_{\text{bound}} = \sqrt{\lambda_H T_H} h_{\text{bound}}. \quad (156)$$

We can also solve the maximum power with given κ , namely, with given u maximizing

$$h(z^*, \sqrt{\frac{u^2+2y}{u^2+2}}, y) = \frac{u(1-\sqrt{\frac{u^2+2y}{u^2+2}})(y-\theta\sqrt{\frac{u^2+2y}{u^2+2}})}{\left(\sqrt{\frac{u^2+2y}{u^2+2}} + \sqrt{y}\right)^2}. \quad (157)$$

The optimal choose of $y^*(u)$ with given u is the root of

$$\begin{aligned} & 2\theta^2 u^2 + y^{3/2}(\theta^2 + 4\theta - 2\theta u^2 - 2u^2) + y^2(-2\theta - 2u^2) \\ & + y(3\theta^2 - 2\theta u^2 + 2u^2) + 4\theta u^2 \sqrt{y} + (-2\theta - 4)y^{5/2} + y^{7/2} - y^3 = 0. \end{aligned} \quad (158)$$

We denote the maximum value as

$$h^* \equiv h(z^*, \sqrt{\frac{u^2+2y}{u^2+2}}, y^*(u)). \quad (159)$$

We use the above results Eqs. (153) and (159) to plot the horizontal gray line and the black dotted curve in Fig. 3 of the main text.

B. Overdamped limit

In the overdamped limit $\kappa^2 \gg \lambda$ or $u \gg 1$, the power Eq. (144) becomes

$$P_{\text{over}}^{\text{slice}} = \sqrt{\lambda_H T_H} h_{\text{over}}(z, y, u), \quad (160)$$

where the function $h_{\text{over}}(z, y, u)$ according to Eq. (150) is

$$h_{\text{over}}(z, y, u) = \frac{1-y}{1-z} \frac{1}{zy-\theta} \frac{1}{u}. \quad (161)$$

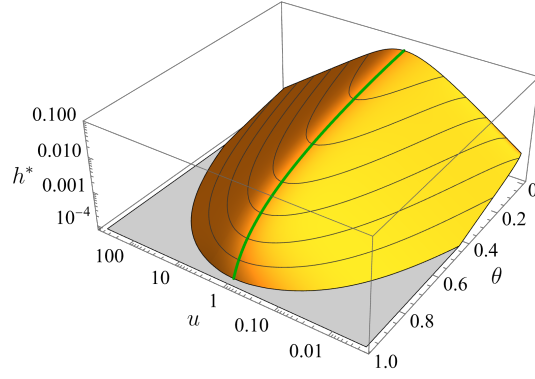


Figure 4. The maximum output power $P^* = \sqrt{\lambda_H} T_H h^*$ as a function of the friction coefficient u and the temperature ratio θ . The green solid curve show the optimal choice of the friction coefficient to maximize the output power $P_{\text{bound}} = \sqrt{\lambda_H} T_H h_{\text{bound}}$. Here we choose $\lambda_H = 1$ and $T_H = 1$.

We have used the fact that $1 - v \approx (1 - y)/u^2$. For $0 < y < 1$ and $\theta/y < z < 1$, the maximum of h_{over} is exactly given by $\phi(\theta)/u$ solved from Eq. (120). And if we consider the sudden quench as the left switching, the dimensionless quantities are explicitly

$$y = \frac{1 + 3\theta}{3 + \theta}, \quad (162)$$

$$z = \frac{3 + \theta}{4}. \quad (163)$$

The output power of the slice cycle then coincides with the approximate result Eq. (132).

C. Underdamped limit

In the underdamped limit $\kappa^2 \ll \lambda$ or $u \gg 1$, the power Eq. (144) becomes

$$P_{\text{under}}^{\text{slice}} = \sqrt{\lambda_H} T_H h_{\text{under}}(z, y, u), \quad (164)$$

where the function $h_{\text{under}}(z, y, u)$ according to Eq. (150) is

$$h_{\text{under}}(z, y, u) = \frac{(1 - \sqrt{y})(1 - z)(\sqrt{y}z - \theta)}{\sqrt{y} - \theta} u. \quad (165)$$

We have used the fact that $v \approx y$. For $\theta^2 < y < 1$ and $\theta/\sqrt{y} < z < 1$, the maximum of h_{under} is

$$h_{\text{under}}^* = \frac{1}{4} u (1 - \sqrt{\theta})^2, \quad (166)$$

which is reached by $y = \theta$ and $z = (1 + \sqrt{\theta})/2$. The output power then coincides with Eq. (67).

D. Maximum output power in general damped situation

We show the maximum output power $P^* = \sqrt{\lambda_H} T_H h^*$ as a function of the friction coefficient u and the temperature ratio θ in Fig. 4. For given θ , large output power can be obtained by choosing an appropriate friction ratio reflecting by u . The bound of the output power $P_{\text{bound}} = \sqrt{\lambda_H} T_H h_{\text{bound}}$ is shown by the green solid curve. Here we choose $\lambda_H = 1$ and $T_H = 1$. The definitions of h_{bound} and h^* are given by Eqs. (153) and (159).

[1] L. S. Pontryagin, V. G. Boltyanskii, R. V. Gamkrelidze, and E. F. Mishechenko, *The Mathematical Theory of Optimal Processes* (Wiley, New York, 1962).

- [2] Z. Gong, Y. Lan, and H. Quan, *Phys. Rev. Lett.* **117**, 180603 (2016).
- [3] A. Dechant, N. Kiesel, and E. Lutz, *Europhys. Lett.* **119**, 50003 (2017).
- [4] D. S. P. Salazar, *Phys. Rev. E* **101**, 030101 (2020).
- [5] Y. H. Chen, J.-F. Chen, Z. Fei, and H. T. Quan, *Phys. Rev. E* **106**, 024105 (2022).
- [6] T. Schmiedl and U. Seifert, *Phys. Rev. Lett.* **98**, 108301 (2007).
- [7] T. Schmiedl and U. Seifert, *Europhys. Lett.* **81**, 20003 (2007).